

Distribution Agreement

In presenting this thesis as a partial fulfillment of the requirements for a degree from Emory University, I hereby grant to Emory University and its agents the non-exclusive license to archive, make accessible, and display my thesis in whole or in part in all forms of media, now or hereafter now, including display on the World Wide Web. I understand that I may select some access restrictions as part of the online submission of this thesis. I retain all ownership rights to the copyright of the thesis. I also retain the right to use in future works (such as articles or books) all or part of this thesis.

Victor Z. Chen

April 12, 2022

YB-1 Post-Transcriptionally Regulates PLXND1 to Mediate Metastasis
in Sonic Hedgehog Medulloblastoma

by

Victor Z. Chen

Dr. Anna M. Kenney

Advisor

Department of Biology

Dr. Anna M. Kenney

Advisor

Dr. Sumin Kang

Committee Member

Dr. Astrid Prinz

Committee Member

2022

YB-1 Post-Transcriptionally Regulates PLXND1 to Mediate Metastasis
in Sonic Hedgehog Medulloblastoma

By

Victor Z. Chen

Dr. Anna M. Kenney

Advisor

An abstract of
a thesis submitted to the Faculty of Emory College of Arts and Sciences
of Emory University in partial fulfillment
of the requirements of the degree of
Bachelor of Science with Honors

Department of Biology

2022

Abstract

YB-1 Post-Transcriptionally Regulates PLXND1 to Mediate Metastasis in Sonic Hedgehog Medulloblastoma

By Victor Z. Chen

Medulloblastoma (MB) is one of the most common brain malignancies in children, accounting for nearly 10% of all pediatric brain tumors. The Sonic Hedgehog (SHH) subgroup, which accounts for 30% of MB cases, is characterized by tumor formation via perturbations in SHH signaling during early cerebellar development. Current treatment options are limited to surgical resection, craniospinal irradiation, and chemotherapy. This standard of treatment yields a ~60-70% survival rate with a high-risk of long-term detriments and reduced quality of life. A significant portion of mortalities from MB are caused by metastatic incidence or recurrence. Our study seeks to investigate potential molecular drivers of metastatic progression in SHH MB. Using *in vitro* primary mouse models and cell lines, we identify Y-box-binding protein 1 (YB-1) as a positive modulator of Plexin D1 (PLXND1) expression. Our studies suggest that YB-1 post-transcriptionally regulates PLXND1 to mediate cell migration, invasion, and tumor development. These findings point to this novel YB-1/PLXND1 signaling axis as a potentially relevant target for metastatic inhibition in SHH MB.

YB-1 Post-Transcriptionally Regulates PLXND1 to Mediate Metastasis
in Sonic Hedgehog Medulloblastoma

By

Victor Z. Chen

Dr. Anna M. Kenney

Advisor

A thesis submitted to the Faculty of Emory College of Arts and Sciences
of Emory University in partial fulfillment
of the requirements of the degree of
Bachelor of Science with Honors

Department of Biology

2022

Acknowledgements

I would like to thank my direct mentor Leon McSwain for lending me the preliminary findings to pursue this project and for always encouraging me to be passionate about science. I am forever grateful for his dedication towards my growth as a scholar. I would like to thank Dr. Kenney for her tremendous support throughout the past three years and for helping me throughout all of my undergraduate research endeavors. Her advice never fails to motivate me. I would like to thank Dr. Prinz for serving as both a member of my committee and as a dedicated advisor and mentor throughout my entire undergraduate career. I would like to thank Dr. Kang for lending me her expertise and providing me with insightful commentary on my project. Special thanks to Dr. Haritha Kunhiraman, Dr. Shubin Shahab, and all the other members of the Kenney Lab for their help with experimental protocols and valuable insights. Lastly, I would like to thank all of my friends and colleagues for providing me with support and encouragement throughout this entire process. This work was supported by the Emory College URP Independent Grant, the URP SURE Fellowship, and the NIH R01 NS110386-01A1 Grant.

Table of Contents

Abstract	4
Acknowledgements	6
Introduction	8
Materials and Methods	12
Results	16
Discussion	19
Figures	21
Figure 1: Schematic depiction of YB-1/PLXND1-mediated metastasis	21
Figure 2: YB-1 positively modulates PLXND1 expression at the post-transcriptional level.....	22
Figure 3: PLXND1 is expressed in SHH MB.....	23
Figure 4: Silencing PLXND1 reduces tumor cell migration.....	24
Figure 5: Silencing PLXND1 reduces tumor cell invasion.....	25
Figure 6: PLXND1 drives select EMT marker expression.....	26
References	27

YB-1 Post-Transcriptionally Regulates PLXND1 to Mediate Metastasis in Sonic Hedgehog Medulloblastoma

Victor Z. Chen¹, Leon F. McSwain², Haritha Kunhiraman², Anna M. Kenney²

¹Department of Biology, Emory College of Arts and Sciences

²Department of Pediatrics, Oncology Division, Emory University School of Medicine

Introduction:

Medulloblastoma (MB) is one of the most common malignant brain cancers in children, accounting for nearly 10% of all pediatric brain tumors¹⁻³. These tumors, which initially form from the cerebellum, are widely thought to arise from the misregulation of genes and pathways involved in postnatal cerebellar development⁴. MB is heterogeneously classified into four subgroups based on differing molecular and histologic characteristics: Wingless (WNT), Sonic Hedgehog (SHH), Group 3, and Group 4⁵. The SHH subgroup, which accounts for 30% of MB cases, is characterized by tumor development via perturbations in the Sonic Hedgehog (SHH) signaling pathway, a major developmental regulator of cell differentiation and proliferation^{4,6}. During postnatal cerebellar development, secretion of SHH morphogenic factor by Purkinje cells sustains the proliferation of select early neuronal progenitor cells⁷⁻⁹. These progenitors, also known as cerebellar granule neural precursors (CGNP), are the putative cells-of-origin for SHH MB^{10,11}. Under normal developmental conditions, the maturation of CGNPs results in the formation of the external granular layer of the cerebellar cortex. However, the misregulation of SHH signaling in these cells can lead to aberrant CGNP development and, subsequently, tumor formation¹².

The current treatment regimen for MB typically includes surgical resection followed by a combination of craniospinal irradiation and adjuvant chemotherapies¹³⁻¹⁵. With this standard of treatment, the 5-year event-free survival rate is ~60-70%^{16,17}. However, these intensive treatments pose a high risk of long-term detriments for pediatric patients and can greatly reduce the quality of life^{18,19}. Furthermore, tumor recurrence is almost universally fatal²⁰. A significant portion of MB mortality results from metastatic dissemination of the primary tumor via leptomeningeal spread²¹. The two main anatomical routes for metastasis in MB include (1) passive diffusion through the cerebrospinal fluid followed by distal leptomeningeal re-implantation and (2) hematogenous extra-neural circulation followed by re-entry into the leptomeningeal space²². Molecular analysis studies have suggested roles for RAS/MAPK, PI3K/AKT, NOTCH, and HGF/cMET signaling in MB metastasis²³⁻²⁶. However, because the majority of research on MB therapeutic strategies thus far has focused on targeting of the primary tumor, the molecular mechanisms driving MB metastasis are not well understood. Therefore, there is a need to identify and elucidate molecular drivers of MB metastatic progression.

A potential target that our group has previously identified as a driver of MB oncogenesis is Y-box-binding protein 1 (YB-1), a DNA- and RNA-binding protein implicated in many cancer-associated cellular processes including cell proliferation, cell cycle control, genomic stabilization, angiogenesis, metabolic regulation, and metastatic progression²⁷. In the past, we have reported YB-1 elevation across all subgroups of MB. Furthermore, we have shown it to be a downstream target of SHH signaling and demonstrated its induction as a requirement for sustaining CGNP and medulloblastoma cell (MBC) proliferation²⁸. Studies performed in bladder, breast, carcinoma, and prostate cancer models have shown a reduction of invasive properties

upon silencing YB-1 expression, and the overexpression of YB-1 has been reported to promote metastasis²⁹⁻³¹. The roles of YB-1 in regulating epithelial-mesenchymal transition (EMT) and maintaining stemness in other models suggest possible mechanisms by which it promotes metastatic progression³². However, the mediation of metastasis by YB-1 has yet to be studied in a MB model.

Due to its ability to bind RNA, YB-1 is involved in various post-transcriptional regulatory processes such as pre-mRNA splicing, mRNA processing and stabilization, mRNP packaging, and translational turnover³³. The dysregulation of RNA-binding proteins (RBP) such as YB-1 may disrupt post-transcriptional control over gene expression, leading to the altered expression and activity observed in many different cancer phenotypes³⁴. Given the significance of YB-1 in MB development, we proposed the dysregulation of YB-1 followed by altered post-transcriptional regulation of oncogenic transcripts as a possible pathway for MB formation. Recent preliminary RNA-binding data from our group identified various novel targets of YB-1 post-transcriptional regulation. One of the targets we identified was Plexin D1 (PLXND1), a transmembrane receptor protein that is classically known for guiding developmental programs during axon growth and vascularization³⁵. PLXND1 signaling via activation by its canonical ligand Semaphorin 3E (SEMA3E) has been shown to drive invasion and metastatic progression in colon cancer, and PLXND1 knockdown has been reported to reduce metastasis in xenograft models³⁶. Furthermore, SEMA3E/PLXND1-mediated EMT has been shown in an ovarian endometrioid cancer model³⁷. Although PLXND1 has yet to be studied in the context of MB, its role during early neuronal development and its involvement in promoting metastasis may prove it to be a potential target of interest for SHH MB.

In the present study, we sought to explore the possibility of YB-1/PLXND1-mediated metastasis in SHH MB. We hypothesized that dysregulation of YB-1 leads to aberrant post-transcriptional modulation of PLXND1, thereby facilitating metastatic progression. To demonstrate this, we investigated (1) the effect of YB-1 modulation on PLXND1 expression and (2) the functional significance of PLXND1 expression in metastatic progression (Fig. 1). We elucidated a YB-1/PLXND1 modulatory association by measuring changes in PLXND1 mRNA and protein expression upon silencing YB-1. Following this, we explored PLXND1 expression in an SHH MB model and tested the functional consequences of knocking down PLXND1 expression on cell migration, invasion patterns, and epithelial-mesenchymal transition (EMT) regulation. Our findings suggest that YB-1 positively modulates PLXND1 at the post-transcriptional level to promote tumor migration, invasion, and development in SHH MB.

Materials and Methods:

Animal Studies

NeuroD2-SmoA1 mice were obtained from Jackson Research Laboratories^{38,39}. Breeding, maintenance, and tumor harvest were carried out in compliance with guidelines from the Emory University Institutional Animal Care and Use Committee.

Primary MB Cell Culture

Medulloblastoma cells (MBC) were isolated from NeuroD2-SmoA1 mouse tumors. Cells were seeded on Matrigel (Corning) coated plates with Neurobasal medium containing penicillin and streptomycin, 1 mmol/L sodium pyruvate, 1x B27 supplement, and 2 mmol/L L-glutamine. Primary MBCs were cultured for 4 hours with 10% fetal bovine serum (FBS) prior to a media change to 0% FBS, at which point lentivirus was added with an incubation time of 48 hours prior to experiment initiation.

Immunofluorescence

Cells were fixed for 10 minutes in fresh 4% Paraformaldehyde prior to 3x wash with PBS. Cells were permeabilized with 0.3% Triton X-100 and blocked with 5% Bovine Serum Albumin and 3% Normal Goat Serum. Primary antibody was added overnight at 4°C and secondary was added for 2 hours at room temperature.

Cell Lines

Mouse MB cell line PZp53Med (PZP) was a generous gift from Dr. Matthew Scott (Stanford)⁴⁰. Human MB cell line ONS-76 was obtained from American Type Culture

Collection. PZP and ONS-76 cells were cultured in DMEM/F12 with 10% FBS. Generation of stable knockdown cell lines was performed through lentiviral delivery of short hairpin constructs followed by puromycin selection. ShSCR and ShSBN were used as negative control constructs for knockdown cell line stabilization. YBX1 knockdown was performed using TRCN0000315309 (referred to as ShYB1-09) in human cell lines and TRCN0000333885 (referred to as ShYB1-85) in mouse cell lines. PLXND1 knockdown was performed using TRCN0000061550 (referred to as ShPLXND1-50) and TRCN0000061552 (referred to as ShPLXND1-52) in human cell lines and TRCN0000078775 (referred to as ShPLXND1-75) and TRCN0000078777 (referred to as ShPLXND1-77) in mouse cell lines (Millipore Sigma).

Western Blotting

Cells were homogenized and lysed in RIPA lysis buffer with protease inhibitors cocktail and phosphatase inhibitors (Thermo Scientific). A total of 15 μ g of each sample was denatured and separated on 6-14% SDS-PAGE gels, then transferred to immobilon-P PVDF membranes (Millipore). Membranes were blocked with 5% milk in tris-buffered saline with 0.1% Tween-20 (TBST). The following primary antibodies were used: YB1 (D299; CST), PLXND1 (NBP1-33634; NOV), β -Tubulin (sc-166729; SCBT), N-Cadherin (D4R1H; CST), β -Catenin (D10A8; CST), Slug (C19G7; CST), Snail (C15D3; CST), Claudin-1 (D5H1D; CST). Anti-Rabbit IgG and Anti-Mouse IgG horseradish peroxidase-conjugated secondary antibodies were used (Jackson ImmunoResearch). Blots were developed with Pierce ECL Western Blotting Substrate and SuperSignal West Pico PLUS Chemiluminescent Substrate (Thermo Scientific). For quantification purposes, chemiluminescent signals were normalized to β -Tubulin. Densitometry was performed using ImageJ software. Acronyms: CST - Cell Signaling Technology, NOV - Novus Biologicals, SCBT - Santa Cruz Biotechnology.

RT-qPCR

RNA was isolated from tissue or cell samples using 1mL TRIzol followed by RNA purification according to the manufacturer's protocol (Thermo Scientific). Reverse transcription was performed on 500ng-2 μ g RNA per 20 μ L RT reaction according to the manufacturer's instructions using a High-Capacity cDNA Reverse Transcription Kit (Applied Biosystems). RT-qPCR was performed using either BioRad 2X SYBR master mix or Applied Biosystems 2X SYBR master mix. 25-200ng of cDNA was utilized per qPCR reaction and primers were validated based on non-template controls and melt-curve analyses. For quantification purposes, C_t values were normalized to β -Actin. Relative expression was calculated using the $\Delta\Delta C_t$ method. The following primer pairs were used:

Species	Target	Forward Primer	Reverse Primer
Human	β -Actin	5' AGA GCT ACG AGC TGC CTG AC 3'	5' AGC ACT GTG TTG GCG TAC AG 3'
	PLXND1	(BioRad qHsaCID0007287)	(BioRad qHsaCID0007287)
	YBX1	5' CCC CAG GAA GTA CCT TCG C 3'	5' GTT CCT TCC TCG GAT GGT CAG 3'
Mouse	β -Actin	5' CCA GTT GGT AAC AAT GCC ATG 3'	5' GGC TGT ATT CCC CTC CAT CG 3'
	PLXND1	5' CGC AAC CGT AGC CTA GAA GAC 3'	5' GGT TAA GGT CGA AGG TGA AGA G 3'
	YBX1	5' CAG ACC GTA ACC ATT ATA GAC GC 3'	5' ATC CCT CGT TCT TTT CCC CAC 3'

Cell Migration and Invasion Assay

Cell migration was measured using *in vitro* wound-healing assays. Cells were seeded with 2.5% FBS and grown to ~70-80% confluence before scratching with a sterile P1000 pipette tip. Wound closure was photographed at 0, 16, 24, and 48 hours post-scratch. Wound closure area was measured using ImageJ software. Cell invasion was measured using 3D colony formation assays in Matrigel (Corning). Cells were embedded in 50% Matrigel and incubated with media replacement every 3 to 4 days. Colony formation was photographed at 14 days post-plating.

Statistical Analysis

Statistical comparisons were performed using GraphPad Prism. One-way analysis of variance (ANOVA) was used for western blotting densitometry, and two-way ANOVA was used for wound-healing analyses. Paired t-tests were used for RT-qPCR analyses. All error bars represent data range. A significance threshold of $p < 0.05$ was used in all analyses.

Results:***YB-1 post-transcriptionally modulates PLXND1 expression***

The identification of novel targets for YB-1 post-transcriptional regulation was accomplished using RNA immunoprecipitation techniques followed by high-throughput RNA sequencing. This analysis demonstrated PLXND1 mRNA to be one of the most differentially enriched transcripts in the entire YB-1 RNA-binding profile (Fig. 2a). We followed up this finding by performing western blot analysis to measure changes in PLXND1 protein expression upon silencing YB-1. Using human-derived SHH MB cell line ONS-76 and mouse-derived SHH MB cell line PZp53Med (PZP), we demonstrated a significant decrease of PLXND1 protein expression in YB-1 knockdown (KD) cells compared to negative control cells (Fig. 2b and 2c). Finally, we paired this immunoblotting data with matched mRNA expression analysis using quantitative reverse transcription PCR (RT-qPCR). In both cell lines, we found no significant changes in PLXND1 RNA expression in YB-1 KD cells relative to the negative control cells (Fig. 2d). These data suggest a positive modulatory effect of YB-1 on PLXND1. Furthermore, they support the idea that this regulation is limited to the post-transcriptional level.

PLXND1 is expressed in SHH MB

PLXND1 expression in SHH MB was measured through microarray gene expression analysis using a profiling array consisting of 763 primary MB patient samples (GEO accession GSE85217). Analysis showed higher levels of PLXND1 gene expression in SHH tumors compared to WNT-activated, Group 3, and Group 4 tumors (Fig. 3a). We corroborated this finding by performing immunofluorescence (IF) staining in primary SHH medulloblastoma cells (MBCs) derived from NeuroD2-SmoA1 transgenic mice (Fig. 3b). Finally, we compared

PLXND1 protein expression between primary MB tumor tissue and matched non-tumor cerebellar tissue (Fig. 3c and 3d). We observed significant enrichment of PLXND1 in tumor tissue relative to cerebellar tissue. These data show PLXND1 to be robustly expressed in a SHH MB model.

Silencing PLXND1 reduces cell migration

To demonstrate the functional role of PLXND1 in cell migration in a SHH MB model, we performed *in vitro* wound-healing assays using PLXND1 stable knockdown cells in both ONS-76 (ShPLXND1-50 & ShPLXND1-52) and PZP (ShPLXND1-75 & ShPLXND1-77) cell lines (Fig. 4a). Within timepoints, we observed markedly reduced wound closure in PLXND1 KD cells compared to negative control cells for both cell lines (Fig. 4b). In ONS-76 cells, knockdown of PLXND1 in the ShPLXND1-50 and ShPLXND1-52 stable cell lines reduced wound closure by an average of 37.4% and 36.6% respectively by the 24-hour timepoint. In PZP cells, wound closure was reduced by 27.9% and 27.8% by the 16-hour timepoint respectively for ShPLXND1-75 and ShPLXND1-77 cells. These findings strongly suggest a role of PLXND1 in promoting cell migration in the context of SHH MB.

Silencing PLXND1 reduces cell invasion

To demonstrate the functional role of PLXND1 in tumor cell invasion in a SHH MB model, we performed 3D colony formation assays and assessed morphological differences between ONS-76 negative control and PLXND1 KD cells (Fig. 5a). Upon imaging 14 days post-plating, we observed considerably reduced branching morphology in PLXND1 KD cells relative to negative control cells. From the total cell count, we calculated 19.9% invasion in the knockdown cells versus 61.2% invasion in the control cells (Fig. 5b). This data supports the role

of PLXND1 in mediating metastatic progression in a SHH MB model by promoting aggressive tumor cell invasion.

PLXND1 drives select EMT marker expression

To demonstrate how PLXND1 may be driving tumor development, we explored the effect of PLXND1 knockdown on the regulation of epithelial-mesenchymal transition (EMT), a set of developmental mechanisms activated during embryogenesis and organ development⁴¹. The deregulation of these developmental mechanisms is seen in many different tumor pathologies as it gives rise to enhanced migratory and invasive capacities⁴². Upon silencing PLXND1 in ONS-76 and PZP cell lines, we measured changes in protein expression for various biomarkers of EMT (Fig. 6a & 6b). In both cell lines, we observed a reduction in mesenchymal markers N-cadherin and β -catenin, two protein regulators of cell-to-cell adhesion^{43,44}. In ONS-76, we also observed decreases in EMT-promoting transcription factors Slug and Snail as well as an increase in Claudin-1, an epithelial tight junction complex protein^{45,46}. While these findings were consistent with our hypothesis of PLXND1 driving a pro-migratory phenotype, changes in Slug, Snail, and Claudin-1 were not recapitulated from cell line to cell line. For PLXND1 KD cells in PZP, we observed increases in Slug and Snail as well as little to no change in Claudin-1. Together, these findings suggest that PLXND1 drives EMT marker expression, and the extent of this regulation may be cell line-dependent.

Discussion:

In this study, we extend previous findings of YB-1 as a driver of tumor development for MB. Our results demonstrate the role of YB-1 as an additional promoter of metastatic progression, a finding that has been reported elsewhere in other cancer models but only now validated in SHH MB²⁹⁻³¹. Through the elucidation of a positive modulatory association between YB-1 and PLXND1, we establish a regulatory mechanism by which YB-1 regulates oncogenic gene expression. We show that silencing YB-1 elicits significant changes in PLXND1 protein expression with non-significant changes in PLXND1 RNA expression. This pinpoints YB-1 regulation on PLXND1 to the post-transcriptional level, emphasizing the significance of YB-1 RNA-binding functions in driving oncogenic phenotypes.

Our findings identify the various functional roles that PLXND1 plays in mediating metastasis in a SHH MB model. We show PLXND1 to be robustly expressed in SHH MB and highly enriched in MB tumor tissue. We recapitulate previously documented phenotypic effects of PLXND1 on metastatic progression by finding significant reductions in migratory and invasive capacity to be functional consequences of silencing PLXND1 activity^{35,36}. Additionally, we demonstrate changes in EMT biomarker expression that are consistent with previous reports of PLXND1 facilitation of mesenchymal marker acquisition and epithelial marker loss in an ovarian cancer model³⁷. However, changes in EMT marker expression for select biomarkers were ambiguous as they were not replicated between ONS-76 and PZP cell lines. While this ambiguity may be the result of exploring EMT regulation in two different systems—one in a human, p53 wildtype cell line and another in a mouse, PTCH receptor-deficient, p53 mutant cell line—, it is noteworthy to point out that EMT analysis was performed using whole-cell lysates. In the case of markers that serve as EMT transcription factors such as Slug and Snail, it may be

more informative to instead study changes in nuclear translocation of these markers upon PLXND1 KD⁴⁷.

While our findings have established a link between YB-1 and PLXND1, further studies are warranted to better understand the detailed mechanism by which YB-1 induces PLXND1 expression. A potential future direction to further refine a regulatory mechanism could be to perform a polysome extraction and profiling experiment to explore the effect of YB-1 on the translational status of PLXND1⁴⁸. One major limitation of our current study is the lack of *in vivo* validation for our functional experiments. A beneficial future study might involve the generation of xenograft mouse models through a knockdown approach of infected MBC implantation followed by observation of metastatic lesions and spread. Additionally, our studies were confined to a single subgroup model for MB. Given previous reports of YB-1 elevation across all 4 subgroups of MB, it might be interesting to extend our studies to other MB subgroups²⁸. This may be especially relevant for Group 3 and Group 4 MB, both of which have higher rates of metastatic incidence and recurrence than SHH-group tumors⁴⁹. Finally, the exploration of PLXND1 binding partners with known therapeutic options may prove to be critical for the targetability of the YB-1/PLXND1 signaling axis for metastatic inhibition⁵⁰. While there are currently no viable options for targeting PLXND1 directly, identifying PLXND1 binding partners and elucidating differentially activated downstream mechanisms may offer alternative and more feasible therapeutic strategy⁵¹. Taken together, our findings point to YB-1/PLXND1-mediated metastasis as a novel and therapeutically relevant area of study for metastatic inhibition in SHH MB.

Figures:

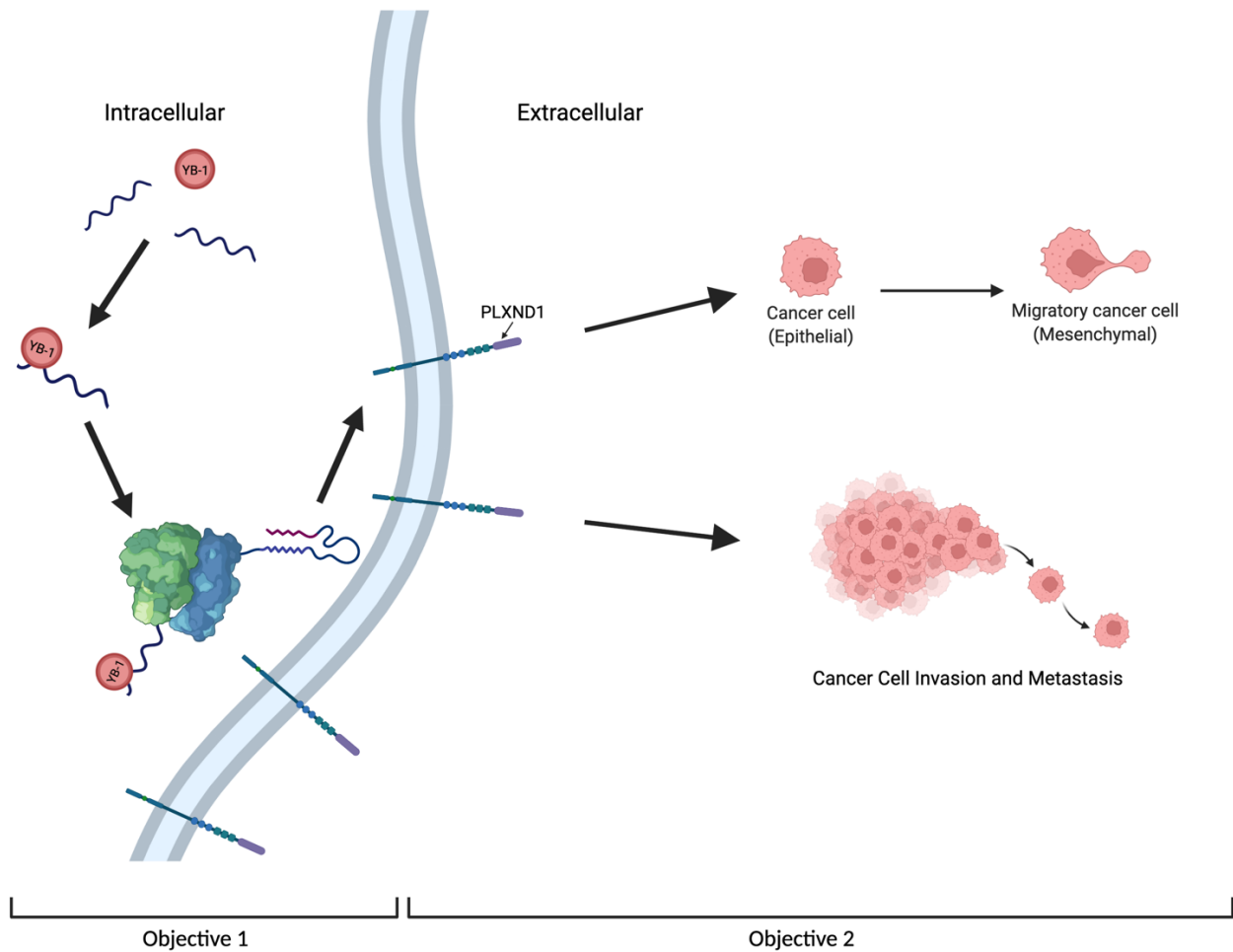


Figure 1. Schematic depiction of YB-1/PLXND1-mediated metastasis. We hypothesized that YB-1 post-transcriptionally regulates PLXND1 to mediate metastatic progression in SHH MB. For Objective 1, we elucidated the effects of YB-1 modulation on PLXND1 expression. For Objective 2, we demonstrated the functional roles of PLXND1 in promoting metastatic phenotypes.

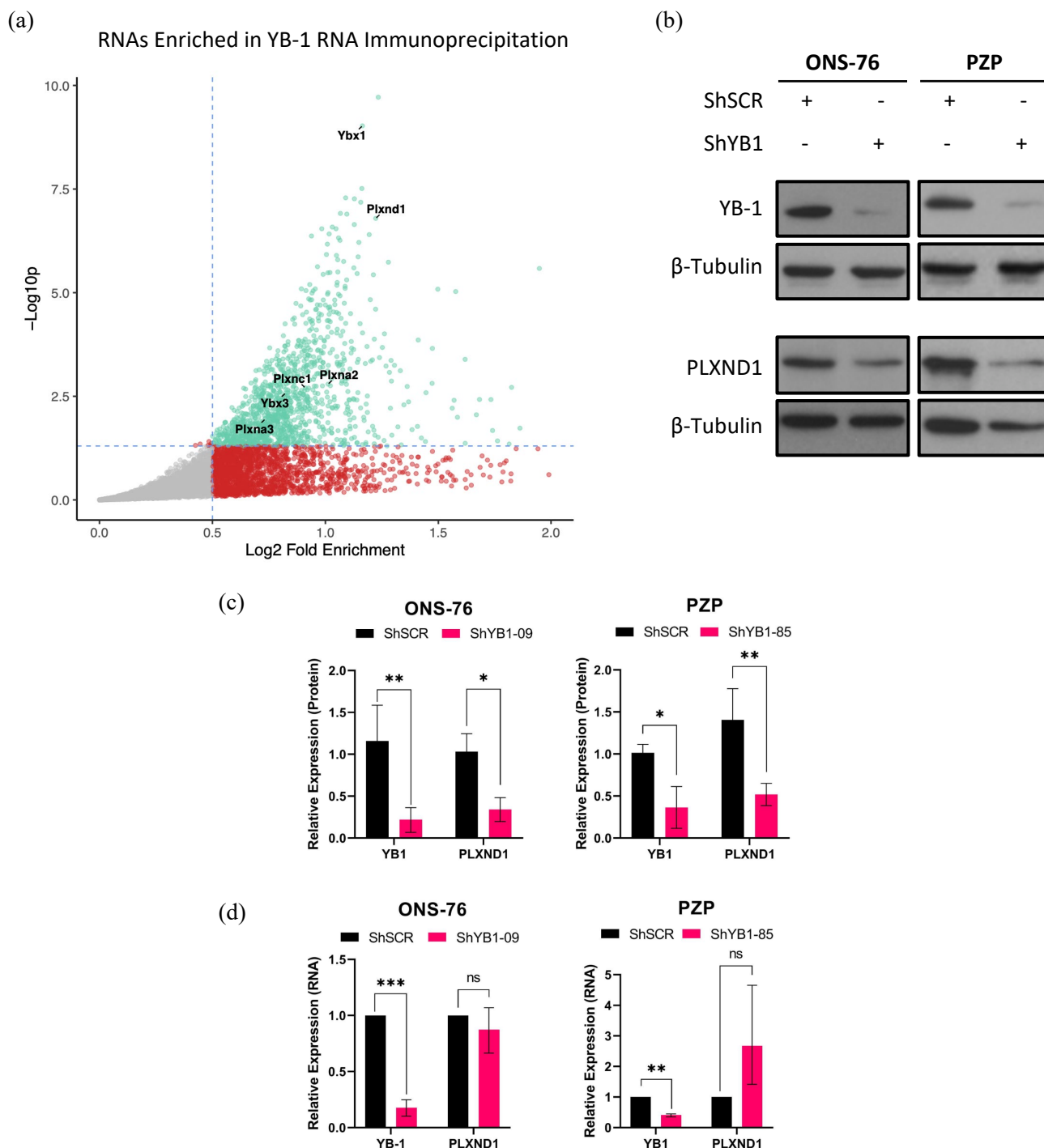


Figure 2. YB-1 positively modulates PLXND1 expression at the post-transcriptional level. (A) Volcano plot of RNA sequencing counts from YB-1 RNA-immunoprecipitation (courtesy of Leon McSwain). YBX1 and YBX3 were used as positive control targets for sequencing analysis. (B) Western blot results demonstrating reduced PLXND1 protein expression upon YB-1 knockdown in ONS-76 and PZP cell lines. ShSCR was used as a negative control for knockdown generation. (C) Western blot densitometry analysis of YB-1 knockdown in ONS-76 (YB-1, $p=0.0034$; PLXND1, $p=0.0150$) and PZP (YB-1, $p=0.0308$; PLXND1, $p=0.0076$). Data are normalized to β -Tubulin, mean \pm range ($n=3$). One-way ANOVA (post hoc, Šidák's multiple comparisons test), * $p\leq 0.05$, ** $p\leq 0.01$. (D) Quantitative reverse transcription PCR (RT-qPCR) analysis demonstrating non-significant changes in PLXND1 RNA expression upon YB-1 knockdown in ONS-76 (YB-1, $p=0.0026$; PLXND1, $p=0.3967$) and PZP (YB-1, $p=0.0028$; PLXND1, $p=0.2364$). Relative expression was calculated as $2^{-\Delta\Delta Ct}$ fold change, mean \pm range ($n=3$). Paired t-test, * $p\leq 0.05$, ** $p\leq 0.01$, *** $p\leq 0.001$.

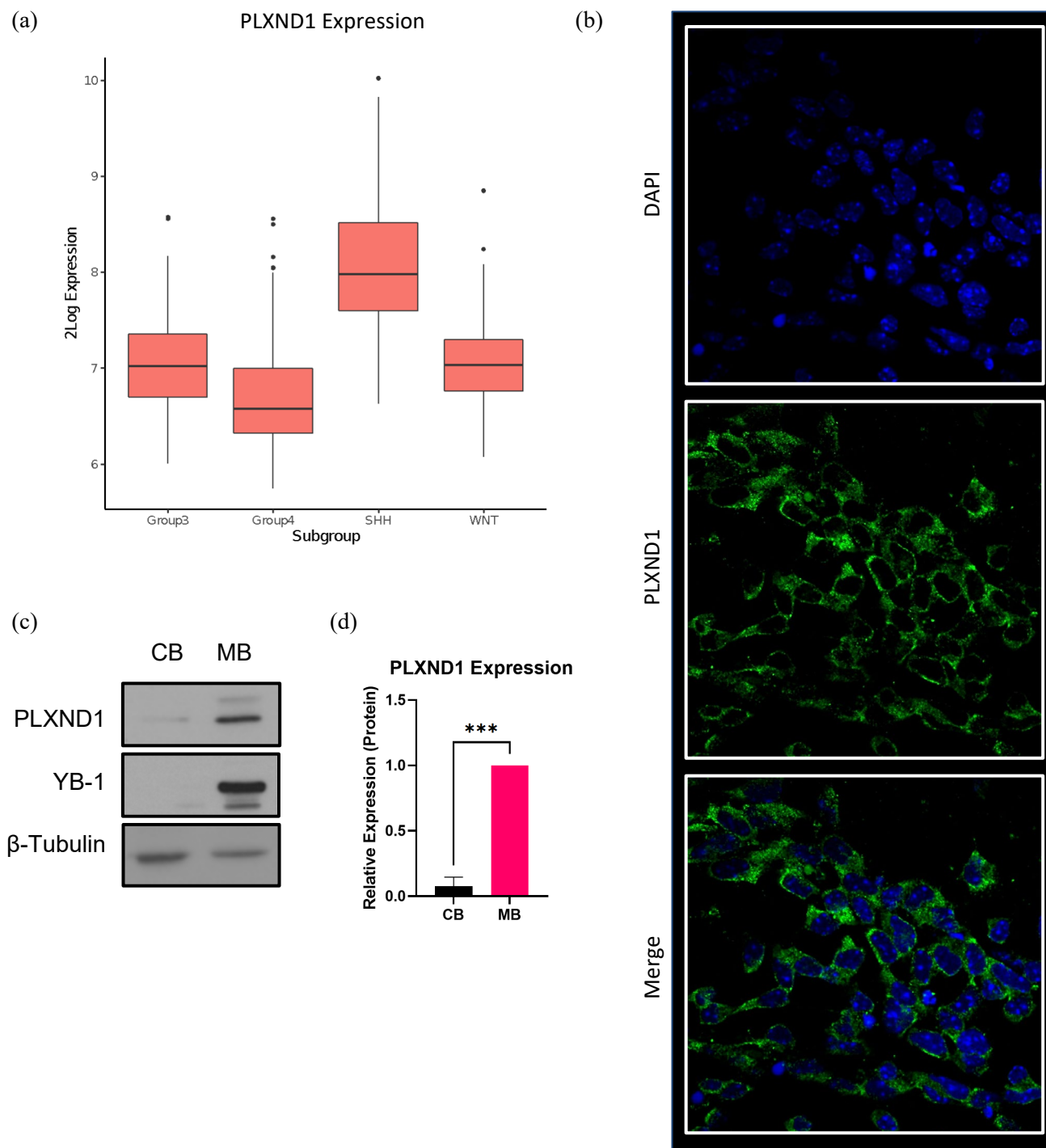


Figure 3. PLXND1 is expressed in SHH MB. (A) Gene expression analysis of PLXND1 in WNT, SHH, Group 3, and Group 4 MB (courtesy of Leon McSwain). Expression data was derived from a previously published microarray profiling set consisting of 763 patient-derived primary MB samples (GEO accession GSE85217). (B) Immunofluorescence staining of primary MBCs derived from NeuroD2-SmoA1 transgenic tumor mice. (C) Western blot results from MB tumor and non-tumor cerebellar tissue from NeuroD2-SmoA1 transgenic tumor mice. (D) Western blot densitometry analysis demonstrating enrichment of PLXND1 in tumor tissue compared to non-tumor tissue ($p=0.0001$). Data are normalized to β -Tubulin, mean \pm range ($n=4$). Paired t-test, $*p\leq 0.05$, $**p\leq 0.01$, $***p\leq 0.001$.

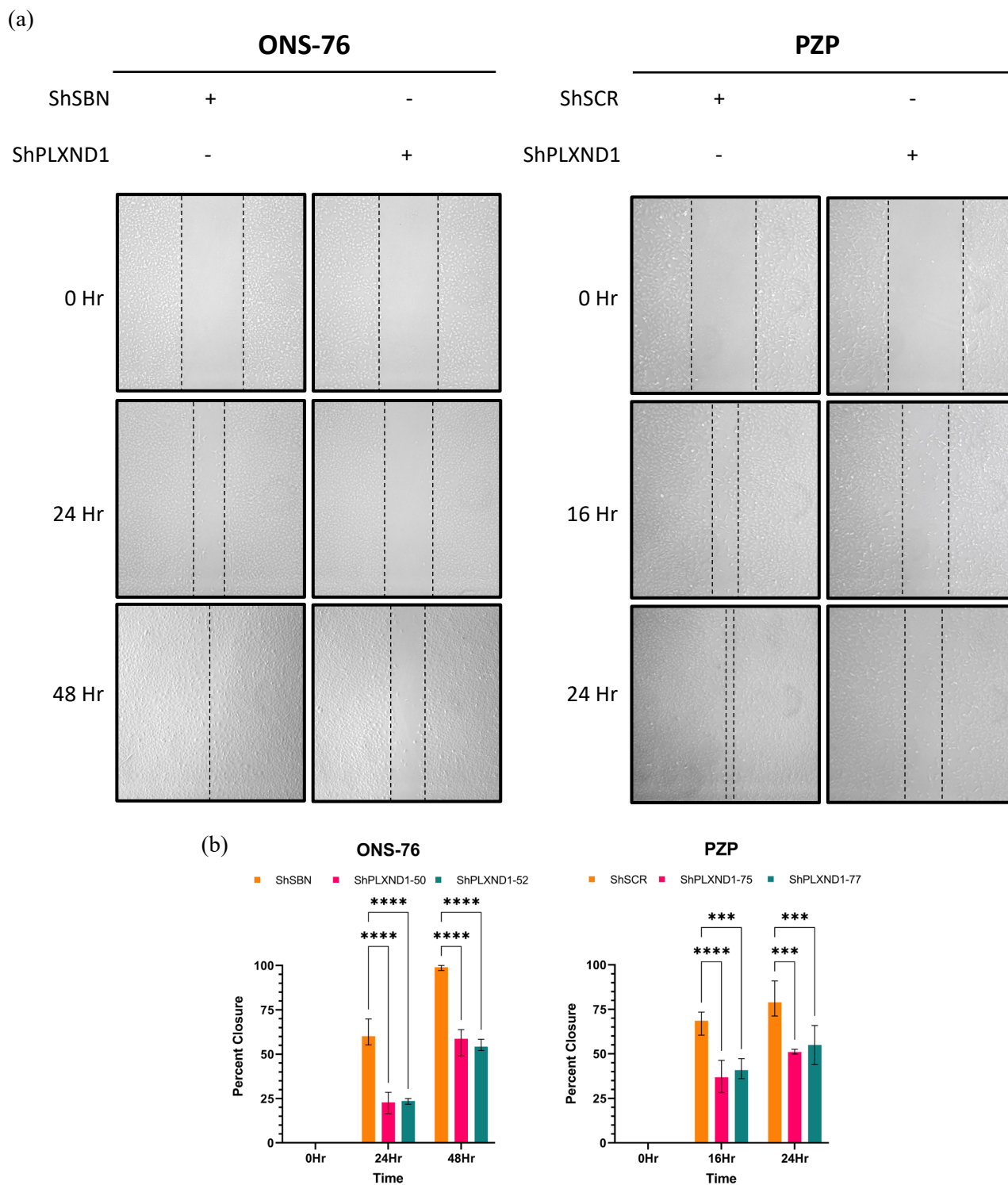


Figure 4. Silencing PLXND1 reduces tumor cell migration. (A) *In vitro* wound healing assays for PLXND1 knockdown in ONS-76 (showing ShPLXND1-50) and PZP (showing ShPLXND1-77) stable cell lines. ShSBN and ShSCR were used as a negative control for knockdown generation. Wounds were imaged at 0, 16, 24, and 48 hours post-scratch. (B) Wound closure analysis demonstrating reduced closure in ShPLXND1-50 (24-Hr, $p < 0.0001$; 48-Hr, $p < 0.0001$), ShPLXND1-52 (24-Hr, $p < 0.0001$; 48-Hr, $p < 0.0001$), ShPLXND1-75 (16-Hr, $p < 0.0001$; 24-Hr, $p = 0.0001$), and ShPLXND1-77 (16-Hr, $p = 0.0001$; 24-Hr, $p = 0.0007$) knockdown cell lines. Percent closure was calculated based on the following formula: $100 - 100 \times (\text{Wound Area} / 0\text{-Hr Wound Area})$, mean \pm range ($n = 3$). Two-way ANOVA (post hoc, Šidák's multiple comparisons test), * $p \leq 0.05$, ** $p \leq 0.01$, *** $p \leq 0.001$, **** $p \leq 0.0001$.

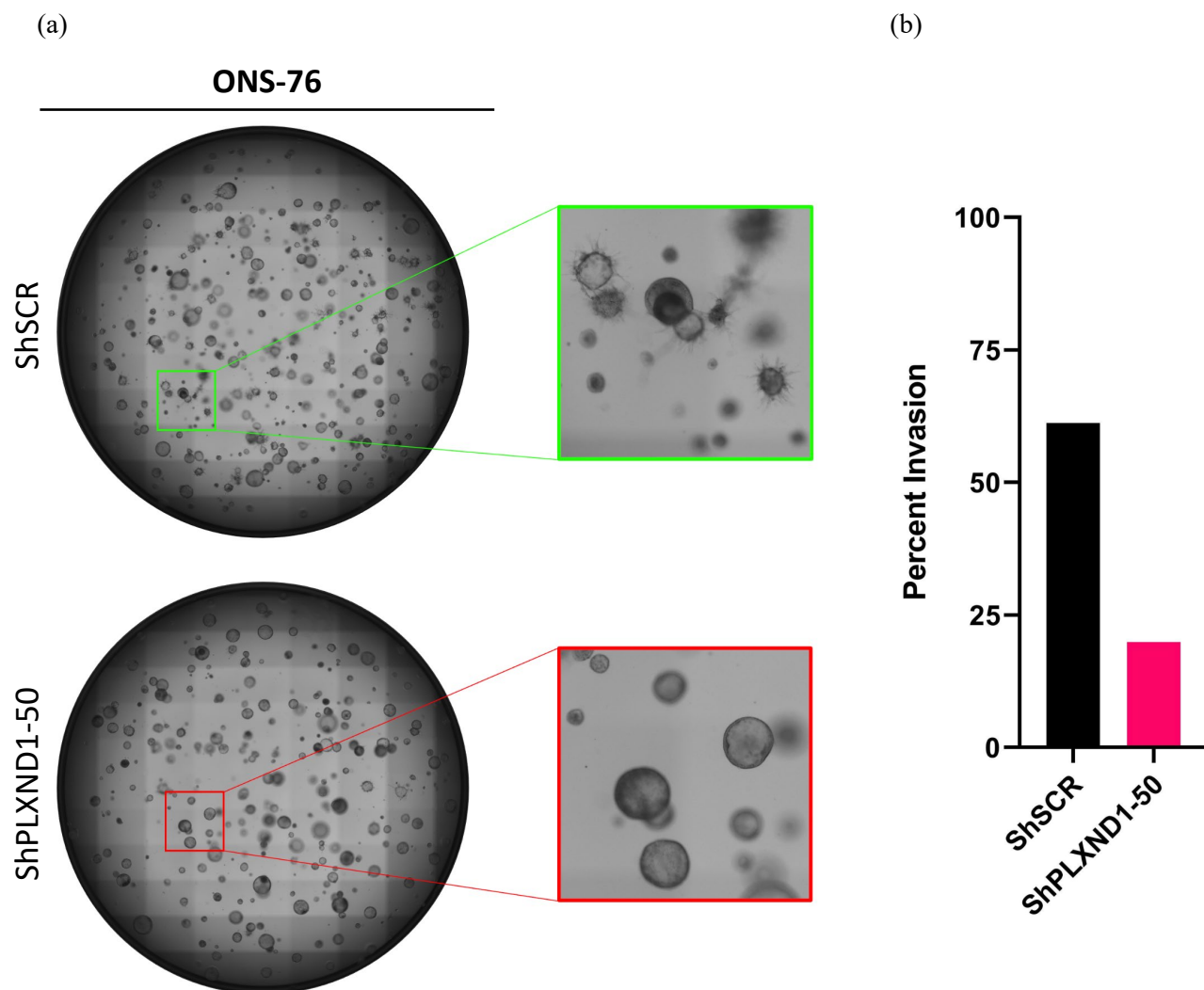


Figure 5. Silencing PLXND1 reduces tumor cell invasion. (A) 3D colony formation assays for PLXND1 knockdown in ONS-76 cell line. ShSCR was used as a negative control for knockdown generation. Colony formation was imaged 14 days post-plating. (B) Colony morphology analysis demonstrating reduced tumor cell invasion in ShPLXND1-50 knockdown cell line (19.9%) compared to ShSCR negative control cell line (61.2%). Percent invasion was calculated based on the following formula: $100 \times (\text{Branched Colony Count} / \text{Total Colony Count})$, (n=1).

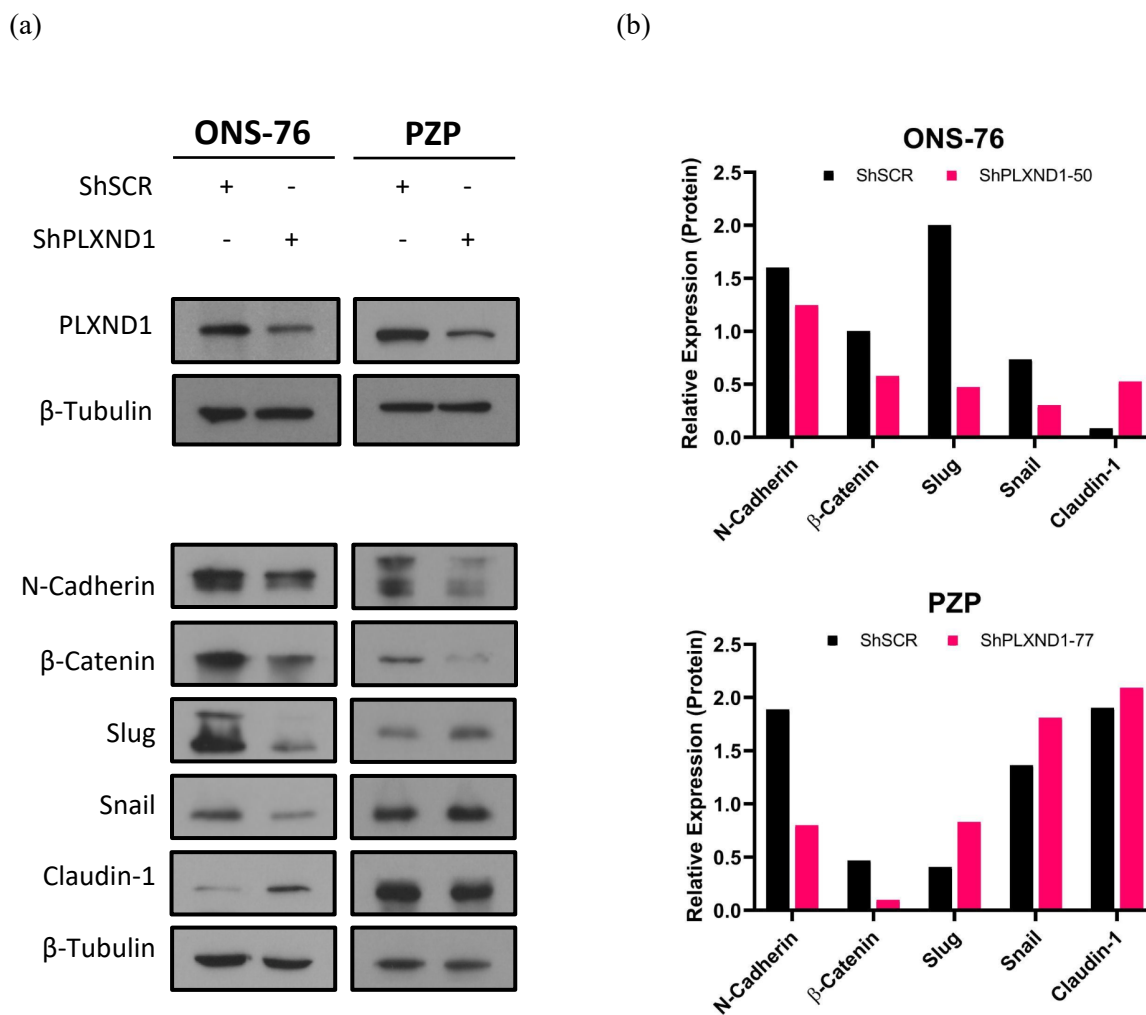


Figure 6. PLXND1 drives select EMT marker expression. (A) Western blot results demonstrating cell line-dependent changes in select epithelial-mesenchymal transition marker expression upon PLXND1 knockdown. ShSCR was used as a negative control for knockdown generation. Mesenchymal markers N-Cadherin, β -Catenin, Slug, and Snail and epithelial marker Claudin-1 were probed in ONS-76 and PZP cell lines. (B) Western blot densitometry analysis of EMT biomarkers in ShPLXND1-50 and ShPLXND1-77 knockdown cell lines. Data are normalized to β -Tubulin, (n=1).

References:

1. Archer TC, Mahoney EL, Pomeroy SL. Medulloblastoma: Molecular Classification-Based Personal Therapeutics. *Neurotherapeutics*. 2017;14(2):265-273.
2. Millard NE, De Braganca KC. Medulloblastoma. *J Child Neurol*. 2016;31(12):1341-1353.
3. Northcott PA, Robinson GW, Kratz CP, et al. Medulloblastoma. *Nat Rev Dis Primers*. 2019;5(1):11.
4. Bihannic L, Ayrault O. Insights into cerebellar development and medulloblastoma. *Bull Cancer*. 2016;103(1):30-40.
5. Northcott PA, Korshunov A, Witt H, et al. Medulloblastoma comprises four distinct molecular variants. *J Clin Oncol*. 2011;29(11):1408-1414.
6. Rimkus TK, Carpenter RL, Qasem S, Chan M, Lo HW. Targeting the Sonic Hedgehog Signaling Pathway: Review of Smoothed and GLI Inhibitors. *Cancers* . 2016;8(2). doi:10.3390/cancers8020022
7. De Luca A, Cerrato V, Fucà E, Parmigiani E, Buffo A, Leto K. Sonic hedgehog patterning during cerebellar development. *Cell Mol Life Sci*. 2016;73(2):291-303.
8. Di Pietro C, Marazziti D, La Sala G, et al. Primary Cilia in the Murine Cerebellum and in Mutant Models of Medulloblastoma. *Cell Mol Neurobiol*. 2017;37(1):145-154.
9. Jeng KS, Chang CF, Lin SS. Sonic Hedgehog Signaling in Organogenesis, Tumors, and Tumor Microenvironments. *Int J Mol Sci*. 2020;21(3). doi:10.3390/ijms21030758
10. Eberhart CG. Even cancers want commitment: lineage identity and medulloblastoma formation. *Cancer Cell*. 2008;14(2):105-107.
11. Behesti H, Marino S. Cerebellar granule cells: insights into proliferation, differentiation, and role in medulloblastoma pathogenesis. *Int J Biochem Cell Biol*. 2009;41(3):435-445.
12. Wallace VA. Purkinje-cell-derived Sonic hedgehog regulates granule neuron precursor cell proliferation in the developing mouse cerebellum. *Curr Biol*. 1999;9(8):445-448.
13. Ashley DM, Merchant TE, Strother D, et al. Induction chemotherapy and conformal radiation therapy for very young children with nonmetastatic medulloblastoma: Children's Oncology Group study P9934. *J Clin Oncol*. 2012;30(26):3181-3186.
14. Gajjar A, Chintagumpala M, Ashley D, et al. Risk-adapted craniospinal radiotherapy followed by high-dose chemotherapy and stem-cell rescue in children with newly diagnosed medulloblastoma (St Jude Medulloblastoma-96): long-term results from a prospective, multicentre trial. *Lancet Oncol*. 2006;7(10):813-820.

15. Thompson EM, Bramall A, Herndon JE 2nd, Taylor MD, Ramaswamy V. The clinical importance of medulloblastoma extent of resection: a systematic review. *J Neurooncol.* 2018;139(3):523-539.
16. Ray S, Chaturvedi NK, Bhakat KK, Rizzino A, Mahapatra S. Subgroup-Specific Diagnostic, Prognostic, and Predictive Markers Influencing Pediatric Medulloblastoma Treatment. *Diagnostics (Basel).* 2021;12(1). doi:10.3390/diagnostics12010061
17. von Bueren AO, Kortmann RD, von Hoff K, et al. Treatment of Children and Adolescents With Metastatic Medulloblastoma and Prognostic Relevance of Clinical and Biologic Parameters. *J Clin Oncol.* 2016;34(34):4151-4160.
18. King AA, Seidel K, Di C, et al. Long-term neurologic health and psychosocial function of adult survivors of childhood medulloblastoma/PNET: a report from the Childhood Cancer Survivor Study. *Neuro Oncol.* 2017;19(5):689-698.
19. Veneroni L, Boschetti L, Barretta F, et al. Quality of life in long-term survivors treated for metastatic medulloblastoma with a hyperfractionated accelerated radiotherapy (HART) strategy. *Childs Nerv Syst.* 2017;33(11):1969-1976.
20. Ramaswamy V, Remke M, Bouffet E, et al. Recurrence patterns across medulloblastoma subgroups: an integrated clinical and molecular analysis. *Lancet Oncol.* 2013;14(12):1200-1207.
21. Van Ommeren R, Garzia L, Holgado BL, Ramaswamy V, Taylor MD. The molecular biology of medulloblastoma metastasis. *Brain Pathol.* 2020;30(3):691-702.
22. Garzia L, Kijima N, Morrissy AS, et al. A Hematogenous Route for Medulloblastoma Leptomeningeal Metastases. *Cell.* 2018;173(6):1549.
23. Gilbertson RJ, Clifford SC. PDGFRB is overexpressed in metastatic medulloblastoma. *Nat Genet.* 2003;35(3):197-198.
24. Guerreiro AS, Fattet S, Fischer B, et al. Targeting the PI3K p110alpha isoform inhibits medulloblastoma proliferation, chemoresistance, and migration. *Clin Cancer Res.* 2008;14(21):6761-6769.
25. Kahn SA, Wang X, Nitta RT, et al. Notch1 regulates the initiation of metastasis and self-renewal of Group 3 medulloblastoma. *Nat Commun.* 2018;9(1):4121.
26. Li Y, Guessous F, Johnson EB, et al. Functional and molecular interactions between the HGF/c-Met pathway and c-Myc in large-cell medulloblastoma. *Laboratory Investigation.* 2008;88(2):98-111. doi:10.1038/labinvest.3700702
27. Lasham A, Print CG, Woolley AG, Dunn SE, Braithwaite AW. YB-1: oncoprotein, prognostic marker and therapeutic target? *Biochem J.* 2013;449(1):11-23.

28. Dey A, Robitaille M, Remke M, et al. YB-1 is elevated in medulloblastoma and drives proliferation in Sonic hedgehog-dependent cerebellar granule neuron progenitor cells and medulloblastoma cells. *Oncogene*. 2016;35(32):4256-4268. doi:10.1038/onc.2015.491
29. Astanehe A, Finkbeiner MR, Hojabrpour P, et al. The transcriptional induction of PIK3CA in tumor cells is dependent on the oncoprotein Y-box binding protein-1. *Oncogene*. 2009;28(25):2406-2418.
30. Shiota M, Yokomizo A, Itsumi M, et al. Twist1 and Y-box-binding protein-1 promote malignant potential in bladder cancer cells. *BJU Int*. 2011;108(2 Pt 2):E142-E149.
31. Evdokimova V, Tognon C, Ng T, et al. Translational activation of snail1 and other developmentally regulated transcription factors by YB-1 promotes an epithelial-mesenchymal transition. *Cancer Cell*. 2009;15(5):402-415.
32. Alkrekshi A, Wang W, Rana PS, Markovic V, Sossey-Alaoui K. A comprehensive review of the functions of YB-1 in cancer stemness, metastasis and drug resistance. *Cell Signal*. 2021;85:110073.
33. Lyabin DN, Eliseeva IA, Ovchinnikov LP. YB-1 protein: functions and regulation. *Wiley Interdisciplinary Reviews: RNA*. 2014;5(1):95-110. doi:10.1002/wrna.1200
34. Nag S, Goswami B, Das Mandal S, Ray PS. Cooperation and competition by RNA-binding proteins in cancer. *Semin Cancer Biol*. Published online March 3, 2022. doi:10.1016/j.semcancer.2022.02.023
35. Gay CM, Zygmunt T, Torres-Vázquez J. Diverse functions for the semaphorin receptor PlexinD1 in development and disease. *Dev Biol*. 2011;349(1):1-19.
36. Casazza A, Finisguerra V, Capparuccia L, et al. Sema3E-Plexin D1 signaling drives human cancer cell invasiveness and metastatic spreading in mice (The Journal of Clinical Investigation (2010) 120, 8,(2684-26980. *J Clin Invest*. 2011;121(7):2945.
37. Tseng CH, Murray KD, Jou MF, Hsu SM, Cheng HJ, Huang PH. Sema3E/plexin-D1 mediated epithelial-to-mesenchymal transition in ovarian endometrioid cancer. *PLoS One*. 2011;6(4):e19396.
38. Hallahan AR, Pritchard JI, Hansen S, et al. The SmoA1 mouse model reveals that notch signaling is critical for the growth and survival of sonic hedgehog-induced medulloblastomas. *Cancer Res*. 2004;64(21):7794-7800.
39. Hatton BA, Villavicencio EH, Tsuchiya KD, et al. The Smo/Smo model: hedgehog-induced medulloblastoma with 90% incidence and leptomeningeal spread. *Cancer Res*. 2008;68(6):1768-1776.
40. Berman DM, Karhadkar SS, Hallahan AR, et al. Medulloblastoma growth inhibition by hedgehog pathway blockade. *Science*. 2002;297(5586):1559-1561.

41. Kalluri R, Weinberg RA. The basics of epithelial-mesenchymal transition. *J Clin Invest*. 2009;119(6):1420-1428.
42. Larue L, Bellacosa A. Epithelial–mesenchymal transition in development and cancer: role of phosphatidylinositol 3' kinase/AKT pathways. *Oncogene*. 2005;24(50):7443-7454.
43. Wang B, Li X, Liu L, Wang M. β -Catenin: oncogenic role and therapeutic target in cervical cancer. *Biol Res*. 2020;53(1):33.
44. Sisto M, Ribatti D, Lisi S. Cadherin Signaling in Cancer and Autoimmune Diseases. *Int J Mol Sci*. 2021;22(24). doi:10.3390/ijms222413358
45. Medici D, Hay ED, Olsen BR. Snail and Slug Promote Epithelial-Mesenchymal Transition through β -Catenin–T-Cell Factor-4-dependent Expression of Transforming Growth Factor- β 3. *MBoC*. 2008;19(11):4875-4887.
46. Kyuno D, Yamaguchi H, Ito T, et al. Targeting tight junctions during epithelial to mesenchymal transition in human pancreatic cancer. *World J Gastroenterol*. 2014;20(31):10813-10824.
47. Buyuk B, Jin S, Ye K. Epithelial-to-Mesenchymal Transition Signaling Pathways Responsible for Breast Cancer Metastasis. *Cell Mol Bioeng*. 2022;15(1):1-13.
48. Kapeli K, Yeo GW. Genome-wide approaches to dissect the roles of RNA binding proteins in translational control: implications for neurological diseases. *Front Neurosci*. 2012;6:144.
49. Miranda Kuzan-Fischer C, Juraschka K, Taylor MD. Medulloblastoma in the Molecular Era. *J Korean Neurosurg Soc*. 2018;61(3):292-301.
50. Meyer LAT, Fritz J, Pierdant-Mancera M, Bagnard D. Current drug design to target the Semaphorin/Neuropilin/Plexin complexes. *Cell Adh Migr*. 2016;10(6):700-708.
51. Worzfeld T, Offermanns S. Semaphorins and plexins as therapeutic targets. *Nat Rev Drug Discov*. 2014;13(8):603-621.